

# Underwater Imaging Color Restoration Using Dehazing Priors With Adaptive Color Correction

Justin Chang

**Abstract**—Underwater images often suffer from color degradation due to light attenuation and backscattering effects. Therefore, color restoration is a crucial process for recovering accurate images in underwater environments. In this paper, we implement a dark channel prior to filter the haze effect in underwater images as well as a color correction algorithm to retrieve attenuated colors. We compared with other underwater prior-based efforts and evaluated each approach’s limitations and strengths. Our approach was robust enough to process the wide variation of underwater scenery, ranging from deep sea to shallow coral scenarios. We also demonstrated that implementing an adaptive color filter allowed for more consistent color corrections that recovered the natural image quality along with higher PSNR values.

**Index Terms**—Computational Imaging, Underwater color restoration, Dark channel prior, Adaptive color correction

## 1 INTRODUCTION

With the advancement in remote sensing technologies, underwater imaging is becoming a clearer reality for conservation and exploration purposes. In conservation, recording time-stamped images of corals give a more complete and accurate view of the effects of climate change and its ecological damages. Specifically, deep underwater autonomous vehicles collect vast samples of geological structures for environmental inspection along with historical records of lost shipwrecks and missing airplanes. The applications for underwater imaging is vast and proves useful for multiple purposes; however, unlike in-air scenery, underwater images need to be processed due to light’s high attenuation and backscattering. As a result, captured image suffer from color distortion and low visibility.

In this project, we discuss some of the limitations to image processing for underwater and the proposed method of dealing with such issues. Specifically, for backscattering we propose a dark channel prior approach that alleviates the overall blue/green hazy features. In addition, we then feed the output to an adaptive color correction algorithm that adjusts the intensity values based on how attenuated the color channels are. We then compare the results with some other relevant work and discuss the future potentials for the image processing pipeline.

## 2 RELATED WORK

For underwater imaging color correction, there are three main approaches: learning-based, prior-based, and algorithmic-based. For learning based methods, recent work has been advancing on deep reinforcement learning in combination with Markov Decision Processes to better train the color correction process [1]. Others have also generated synthetic underwater images to overcome the lack of training data and speed up the process of image restoration [2]. Another popular approach is using a model-based environment and uses a convolutional neural network to enhance the images according to various color degradation scenarios [3]. Learning-based efforts have seen great progress in the

field of computational imaging and computer vision, but it’s not the most apt approach because there’s a limited amount of labeled data for underwater images. In addition, cameras are installed in remotely operated vehicle and autonomous vehicles, which are often sent for scientific discovery purposes. With remote monitoring missions, images are often first of its kind so it’s difficult to utilize learning methods when no training data is available.

In addition, a lot of effort has been using prior-based methods for underwater image restoration. The most popular is the dark channel prior, which is based on image intensity statistics of natural haze-free images [4]. In air, correcting backscattering becomes more prevalent with long range outdoor scenes. In underwater vision, the same assumption may be used as water fogs farther objects at a faster rate than in-air. Efforts have been used to adapt the dark channel prior to underwater scenes, such as manipulating the intensities in Red, Green and Blue (RGB) channels [5]. Others have also proposed to select only the Green and Blue channels when working with the prior due to the fact that red color wavelengths are almost entirely attenuated starting from relatively shallow depths [6]. The first of this project’s method focuses on using a dark channel approach to dehaze the images, allowing for better clarity and image restoration. In addition, the works from author [5] and also [6] were also evaluated in Section 4.

Moreover, physics-based algorithms such as the popular Seathru, which identifies correct attenuation coefficients using depth information, have been widely used to recover lost colors in underwater images [7]. Others have also separated the whole pipeline into a two-step process: color correction and optimal contrast [8]. The rest of the project explores work from [9] to help with the color enhancement after the dehazing process.

## 3 PROPOSED METHOD

### 3.1 Problem Formulation

$$E_T = E_d + E_f + E_b \quad (1)$$

The underwater image formation can be summarized with Equation 1 where  $E_T$  is the total radiance the camera sensor receives.  $E_d$  is the radiance reflected from the object. When light reflects, it's also attenuated due to absorption by the water. Depending on the wavelength, light attenuates at different depths. In the visible light spectrum, red intensities get absorbed first, following with green then blue. Figure 1 demonstrates the corresponding depths light becomes absorbed.

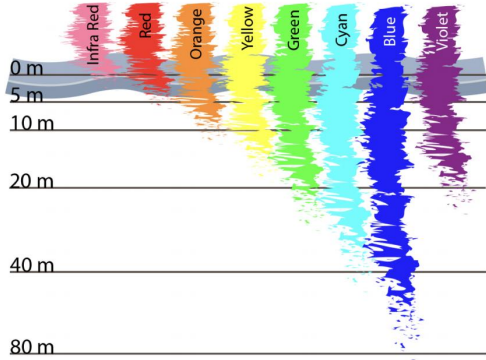


Fig. 1: Light Attenuation underwater. Image provided by [10]

To address the color attenuation, this project focuses on using the color correction algorithm inspired from the authors at [9]. We only adapt the efforts for color compensation and balance as it proved the most effective in restoring the original image. The rest of the author's work focuses on detail enhancement and minor gamma correction using improved retinex algorithm which improves the overall image quality, but doesn't focus on the color balance.

$E_f$  from Equation 1 then refers to forward scattering. Forward scattering happens when the light reflected from the object gets spread out on its way to the camera sensor. As a result, it incurs a blur in the image which is typically described as a convolution blur. Forward scattering has an insignificant effect on the color degradation of the color, hence is not discussed further in the project.

$E_b$  is called backscattering and it happens when there's an ambient light that reflects on particles in the scene, causing it to be captured by the camera. The backscattering effect, or also known as the veiling light, becomes more prevalent as the distance between the camera and the scene gets further. In normal conditions, haze and fog cause ambient light to backscatter during image capturing, hence inducing a degradation color and image visibility. Similarly, the effects of backscattering becomes more obvious in underwater scenarios as the attenuation coefficient in water is higher than in air.

Therefore, a dehazing prior was used for this project to address the backscattering issue. Specifically, the Dark Channel Prior is used to help retrieve the dehazed underwater scene. The details of the Dark Channel Prior is highlighted in section 3.3.

### 3.2 Proposed Processing Pipeline

Since direct attenuation and backscattering affects in tandem color distortion, this project proposes to connect the output of an underwater-ready dark channel prior to the input of color correction. The dark channel prior works like a prefilter for the color correction as it allows the background and overall blue/green "haziness" of the image to be removed first. In addition, recovering the haze-free image first allows for the color correction algorithm to work smoother as it has a cleaner input, which theoretically yields better results. Moreover, the correction algorithm wasn't chosen to be implemented upstream because they often distort the intensity distribution in color channels. Since the prior is mostly a linear operation, downstream color correction should work without major setbacks. Figure 2 shows a high-level view on the project's processing pipeline.

### 3.3 Dark Channel Prior

The model widely used to form haze in the computer vision and graphics field is described in Equation 2.

$$I(x) = J(x)t(x) + A(1 - t(x)) \quad (2)$$

$I(x)$  refers to the observe intensity,  $J(x)$  is the scene radiance,  $t$  is the transmission, and  $A$  is the atmospheric light. The goal of haze removal is to recover  $J(x)$  from the given  $I(x)$  via estimation of the transmission and atmospheric light.

The dark channel prior is based on the statistical observation that in outdoor haze-free images, the lowest intensity among all color channels is close to zero. In other words,

$$J^{dark}(x) = \min_{c \in \{r, g, b\}} (\min_{x \in \Omega} (J^c(y))) \quad (3)$$

Equation 3 shows that within a local patch  $\Omega$  the darkest intensity across all color channels is very low. The phenomenon is based on 1) shadows existing in natural objects and 2) colorful and bright objects tend to have very low intensities in the other color channels. Therefore, Equation 2 simplifies to Equation 4.

$$\min_{x \in \Omega} I^c(x) = \min_{x \in \Omega} J^c(x)\tilde{t}(x) + A(1 - \tilde{t}(x)) \quad (4)$$

The  $\tilde{t}(x)$  refers to the transmission within that patch. Since  $A$  is a constant, it can be divided on both sides to yield Equation 5.

$$\min_{x \in \Omega} \frac{I^c(x)}{A^c} = \min_{x \in \Omega} \frac{J^c(x)}{A^c} \tilde{t}(x) + (1 - \tilde{t}(x)) \quad (5)$$

Taking the min operator on both sides of Equation 5 shows Equation 6.

$$\min_{c \in \{r, g, b\}} \min_{x \in \Omega} \frac{I^c(x)}{A^c} = \min_{c \in \{r, g, b\}} \min_{x \in \Omega} \frac{J^c(x)}{A^c} \tilde{t}(x) + (1 - \tilde{t}(x)) \quad (6)$$

With the dark channel having values close to zero, the first term on the right hand side becomes 0, which allows us to estimate the transmission with the following equation.

$$\tilde{t}(x) = 1 - \min_{c \in \{r, g, b\}} \min_{x \in \Omega} \frac{I^c(x)}{A^c} \quad (7)$$

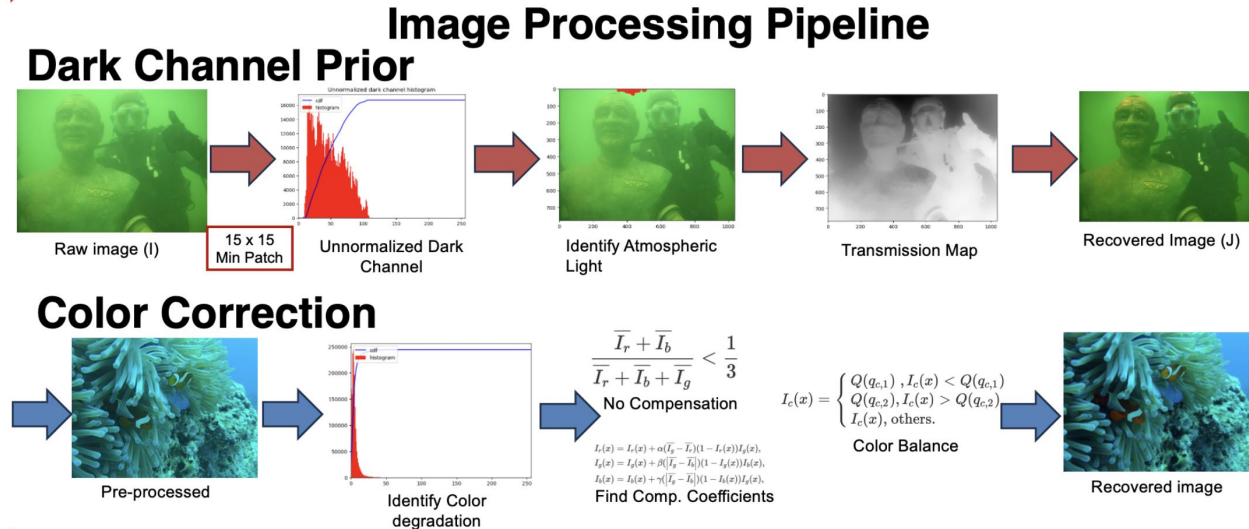


Fig. 2: Proposed Image Processing Pipeline

However, the atmospheric light  $A$  needs to be estimated first. The Dark Channel chooses the brightest 0.1% pixels and identifies that region as the atmospheric light. This procedure is synonymous with choosing the most haze-opaque area and identifying it as the light source. Now that  $A$  is determined,  $t$  can be estimated along with the final scene radiance  $J$ . In certain scenarios the transmission may be really small, which makes the scene radiance subject to noise. To resolve that, we add a parameter  $t_0$  that's usually set to 0.1 to prevent divisions close to zero. Finally, the clean image is recovered using Equation 8.

$$J(x) = \frac{I(x) - A}{\max(t(x), t_0)} + A \quad (8)$$

### 3.3.1 Underwater-specific Dark Channel Priors

This project proposes that the only modification to the dark channels is the atmospheric light estimation. In in-air images, the brightest area corresponds to white; however, in underwater the backscattered light is mostly blue. Therefore, a color shift is proposed with red and green color channels are taken for their complement. Figure 3 demonstrates the color shift to compensate for better atmospheric light estimation. This approach finds inspirations from the work at [10] to shift colors for choosing the correct haze-opaque area.

## 3.4 Color Correction Algorithms

As shown in Equation 1, another aspect that significantly degrades underwater color is direct attenuation  $E_d$ . One approach is the adaptive color correction algorithm inspired from the authors at [9]. To remove color cast, a color compensation and color balance is implemented. First, it looks at whether the mean red and blue channel intensities are heavily distorted. If they are, a color compensation is necessarily performed.

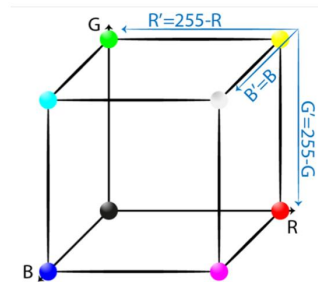


Fig. 3: Color Shift Diagram. Image provided by [10]

### 3.4.1 Color compensation

$$I_r(x) = I_r(x) + \alpha(\bar{I}_g - \bar{I}_r)(1 - I_r(x))I_g(x) \quad (9)$$

$$I_g(x) = I_g(x) + \beta(\bar{I}_g - \bar{I}_b)(1 - I_g(x))I_b(x) \quad (10)$$

$$I_b(x) = I_b(x) + \gamma(\bar{I}_g - \bar{I}_b)(1 - I_b(x))I_g(x) \quad (11)$$

The  $I_{r,g,b}(x)$  are the pixel values of the RGB channels and the  $\alpha, \beta, \gamma$  coefficients are determined based on how attenuated the color channels are with respect to each other. The coefficient values are usually set as the negative log of the differences in the mean intensity of color channels. For specific coefficient finding details, please refer to the paper at [9].

### 3.4.2 Color balance

Once the colors are compensated, they are then compensated based off of quantile pixel values. The quantile pixel values are highlighted in equation 12.  $\tilde{I}_c$  indicates the mean value of the compensated image in its respective channel.

$$q_{c,1} = 0.005 \frac{\max(\tilde{I}_r, \tilde{I}_g, \tilde{I}_b)}{\tilde{I}_c}, q_{c,2} = 1 - q_{c,1} \quad (12)$$

Then each pixel in the color channels are compared element-wise. If the pixel is less than  $q_{c,1}$ , it's set to  $q_{c,1}$ . If



it's greater than  $q_{c,2}$ , it's then set to  $q_{c,1}$ . The value remains the same if otherwise. It then finally goes through a color stretch as detailed in Equation 13.

$$I_c = \frac{I_c - I_{c,min}}{I_{c,max} - I_{c,min}} \quad (13)$$

#### 4 EXPERIMENTAL RESULTS

All sample photos were used from an online underwater image enhancement database found here: [https://li-chongyi.github.io/proj\\_benchmark.html](https://li-chongyi.github.io/proj_benchmark.html). The provided non-commercial dataset has 950 real-world underwater raw and ground truth images.

The first step is implementing the unnormalized dark channel. A  $15 \times 15$  patch loops around all color channels and identifies the lowest intensities. As mentioned in section 3.3.1, the red and green channels are taken for their complement so that the atmospheric light estimation is more realistic for underwater scenery. Figure 4 demonstrates the dark channel histogram of all the pixels and their lowest intensities in the bronze statue reference image. Figure 5 shows the gray-scale version of the same image.

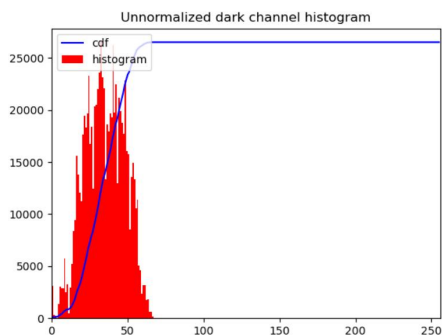


Fig. 4: Dark Channel Histogram



Fig. 5: Gray-scale of Dark Channel

Out of the 0.1% brightest intensity, the brightest pixel is identified as the atmospheric light. Then, the transmission map may be estimated using Equation 7. One thing to note is that the raw transmission map is derived using the patch,

which causes all transmission values within the patch to be the same. A guided filter is therefore implemented to preserve edges and refine the transmission so that the recovered scene radiance retains the original details. In addition, Equation 7 adds an  $\omega$  multiplication term of 0.95 on the right hand side for realistic applications because having a small-scale haze effect allows for better visual recognition and natural depth perception. With that in mind, Figure 6 shows a refined transmission map which can they be used to derive the final scene radiance.



Fig. 6: Refined Transmission Map using Guided Filter

Once the scene radiance is recovered, it's then put into the color correction algorithm. The algorithm first identifies the minimum, maximum, and mean values of each color channel. There's 4 different case scenarios that help with finding the compensation coefficients for Equations 9, 10, and 11. 1) If the difference between the mean blue and green channels is small, the red colors need to be adjusted. 2) If the difference between the mean blue and green is big, it means that the red and green channels needs compensation. 3) If the image is predominantly green, the red and green channels are adjusted. 4) If the scene is mainly yellow, the blue channel is adjusted. The four cases sought to capture the wide variation of underwater scenery and correct the colors in an all-encompassing manner. After the compensation, the images are compared with its quantile pixel value using Equation 12 and finally stretched using Equation 13 for color balance. Figure 7 shows a comparison of the before and after color adjustments.

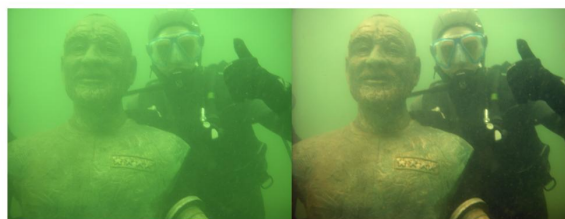


Fig. 7: Color Correction Algorithm Before vs. After

#### 4.1 Correction Algorithm Comparisons

When evaluating the color correction algorithm efficiency, quantitative comparisons become tricky. The ground truth images provided in the database had a wide variance of enhancement effect; some had consistent color readings but most had stark color contrasts that were hard to identify as

effective ground truth images at all. Also, since underwater color correction is an ongoing research field, it's hard to identify which outputs are more trusted than others. Therefore, most comparisons are done qualitatively while quantitative results are provided for images that yielded reasonable ground truth images.



Fig. 8: Color Correction Algorithm Comparison. Column 1: Reference Image. Column 2: Raw Image. Column 3: Approach from [8] Column 4: Our approach

We compared our correction algorithm with a piecewise linear color stretching method [8]. First, the author assumes the average color is achromatic using the gray-world hypothesis. They then stretch the image's mean intensity towards 128 across all channels. If one of the channels is heavily degraded with the average pixel intensity less than 40, it applies another level of hyper-parameter tuning to prevent it from over-correcting.

Figure 8 shows the qualitative comparison for color adjustment outputs. In more green overtones, the approach from [8] corrects the colors really well, as seen with a peak signal to noise (PSNR) value of 20.5 with the bronze statue. The adaptive algorithm still corrected the image, but the overall green tone was still prevalent. The adaptive algorithm reached a PSNR of 17.19, showing that it didn't have an improvement over the author's work at [8].

However, the work from [8] is prone to over-correcting colors. This is seen in the jellyfish with an unnaturally orange/red hue. The red jellyfish had a PSNR of 14.5 while this project's implementation reached 23.8. Because the project aimed to account for the wide range of color distribution for underwater scenes, the adaptive approach was more suitable. In addition, because the color correction was implemented downstream of the dehazing priors, allowing for my flexibility in color distribution was advantageous to yielding consistent results.

#### 4.2 Priors Comparison

Other underwater-specific priors efforts mentioned in section 2 were compared with this project's approach. For example, authors at [6] only considered the green and blue channels for their dark channels since they proposed that red light attenuated so much it was irrelevant for analysis. Their approach is labeled as the Underwater Dark Channel Prior (UDC). The naive dehazer method, which was implemented mainly for in-air foggy images, were also used as a benchtest. Lastly, the dehazing-only method from [10], also known as Underwater Red Dark Channel (UWRDC), is included to demonstrate how effective our project's added color correction algorithm was. The qualitative and PSNR values are shown in figure 9.

When implementing the naive DC, there was almost no effect on underwater scenes. This was to be expected as the atmospheric light estimation relied on estimating the brightest spot as white, which is not the case for this application. The UDC surprisingly over-saturated the image with a blue hue. It also showed with a PSNR of 11.8 that it's output was worse than the raw image. The UWRDC dehazed the background a bit, but the colors were still heavily degraded. This project's approach, which is highlighted in the last column, had a higher PSNR value of 14.9 than the rest of the executions. It also demonstrated better color restoration in the foreground corals as well as dehazing efforts in the background. Overall, the image processing pipeline of combining dehazing efforts with other color correction processes has the most promising outlook for restoring underwater images.

## 5 DISCUSSION

The main issue with simple linear color correction algorithms is that it doesn't work well with the high variance in underwater scenery. Deep sea images with dark overtones hold a stark contrast to the shallow and vibrant coral images. Linear transformations, when treated as a one size fit all, often leads to over-correction and unnatural color distributions. That's why having an adaptive filter that's based on the distribution of colors with respect to other color channel works best among all correction algorithm candidates. Moreover, as seen in figure 8, color corrections algorithms are not tuned well for hazy backgrounds, which supported the project's motivation for applying a prior as a pre-filtering mechanism.

Implementing a prior based approach has its own drawbacks too. The biggest limitation with underwater priors is that it poorly identifies the atmospheric light source. Typically having highly reflective objects, such as sand or coral, disrupts the algorithm in finding out where the global light source is. With a wrong identification of light source, the transmission is miscalculated and ultimately outputs a significantly degraded image. Therefore, some mechanism to identify and filter out misaligned bright objects would be beneficial in seeing better prior-based results.

In addition, a one size fit all approach with priors seems like isn't the best idea moving forward due to the high variance in underwater scenery. Most prior assumes that blue is the predominant color and tries to estimate the atmospheric light with the darkest blue. However, as seen in the UDC in figure 9, it's also prone to over-saturate with that assumption. Therefore, incorporating a more physics and depth-based attenuation coefficient into the transmission map and atmospheric light should show more promising and robust results.

## 6 CONCLUSION

In this paper, we explored implementing a dehazing prior with adaptive color correction to restore color accuracy for underwater scenery. We see that the prior helped alleviate the background hazy features of underwater scenery. In addition, the color restoration process was robust enough to correct for large color channel imbalances. By cascading









Ref.	Raw	Naïve DC	UDC	UWRDC	Ours
					
N/A	13.4	13.4	11.8	13.5	14.9

Fig. 9: Priors Comparison

the dark channel prior with a color correction algorithm, it yielded better qualitative and quantitative results than the other author's works. Our approach showed better color improvement than the naive DC, UDC, and UWRDC priors. In addition, the adaptive algorithm also showed more consistent results than piece-wise linear transformation color correction algorithms. As a future work, devising a mechanism to pre-filter highly reflective objects like sand and corals shows great potential in accurately identifying atmospheric light in underwater scenery, ultimately leading to more robust image processing pipelines.

#### ACKNOWLEDGMENTS

The author would like to thank Professor Gordon Wetzstein for an amazing class on computational imaging. Also thank you for the great guidance for this project.

#### REFERENCES

- [1] S. Sun, H. Wang, X. Wu, L. Li, H. Zhang, M. Li, and P. Ren, "Underwater color correction via deep reinforcement learning," in *OCEANS 2021: San Diego – Porto*, 2021, pp. 1–4.
- [2] K. Cai, Z. Yang, H. Pang, X. Miao, J. He, Y. Liu, T. Zhang, and W. Wang, "A novel underwater color correction method based on underwater imaging model and generative adversarial network," *Computers and Electronics in Agriculture*, vol. 200, p. 107186, 2022. [Online]. Available: <https://www.sciencedirect.com/science/article/pii/S0168169922005038>
- [3] Y. Liu, H. Xu, B. Zhang, K. Sun, J. Yang, B. Li, C. Li, and X. Quan, "Model-based underwater image simulation and learning-based underwater image enhancement method," Apr 2022. [Online]. Available: <https://www.mdpi.com/2078-2489/13/4/187>
- [4] K. He, J. Sun, and X. Tang, "Single image haze removal using dark channel prior," in *2009 IEEE Conference on Computer Vision and Pattern Recognition*, 2009, pp. 1956–1963.
- [5] C.-Y. Cheng, C.-C. Sung, and H.-H. Chang, "Underwater image restoration by red-dark channel prior and point spread function deconvolution," *2015 IEEE International Conference on Signal and Image Processing Applications (ICSIPA)*, pp. 110–115, 2015. [Online]. Available: <https://api.semanticscholar.org/CorpusID:18769392>
- [6] F. M. S. B. P. D. Jr, E. do Nascimento and M. Campos, "Transmission estimation in underwater single images," *2013 IEEE International Conference on Computer Vision Workshop*, pp. 825–830, 2013.
- [7] D. Akkaynak and T. Treibitz, "Sea-thru: A method for removing water from underwater images," in *2019 IEEE/CVF Conference on Computer Vision and Pattern Recognition (CVPR)*, 2019, pp. 1682–1691.
- [8] X. Fu, Z. Fan, M. Ling, Y. Huang, and X. Ding, "Two-step approach for single underwater image enhancement," in *2017 International Symposium on Intelligent Signal Processing and Communication Systems (ISPACS)*, 2017, pp. 789–794.
- [9] S. Lin, Z. Li, F. Zheng, Q. Zhao, and S. Li, "Underwater image enhancement based on adaptive color correction and improved retinex algorithm," *IEEE Access*, vol. 11, pp. 27 620–27 630, 2023.
- [10] T. Luczynski and A. Birk, "Underwater image haze removal and color correction with an underwater-ready dark channel prior," *CoRR*, vol. abs/1807.04169, 2018. [Online]. Available: <http://arxiv.org/abs/1807.04169>